COBEM 2021 26th International Congress of Mechanical Engineering
November 22-26, 2021, Virtual Congress, Brazil
ABCM Associação Brasileira de Engenharia e Ciências Mecânicas

COB-2021-0887
DEVELOPMENT AND COMPARISON OF EXPERIMENTAL EMISSIVITY MEASUREMENT METHODS: APPLICATION TO SURFACES FOUND IN OFFSHORE FLARE

Pedro Oliveira
Sergio Leal Braga
Florian Pradelle
Department of Mechanical Engineering, Pontifícia Universidade Católica do Rio de Janeiro (PUC-Rio), Rua Marquês de São Vicente, 225, Gávea, Rio de Janeiro, RJ, CEP:22453-900, BRAZIL
oaken182@gmail.com; slbraga@puc-rio.br; pradelle@puc-rio.br

Zrinka Vidakovic Romani
Equipment Engineering, Petrobras, Av. Henrique Valadares, 28 - 5th floor - Tower A, Downtown, Rio de Janeiro, RJ, CEP:20231-030 ,BRAZIL
zrinka@petrobras.com.br

Abstract. *With the growth of off-shore oil extraction in recent years, particularly from the pre-salt, it is necessary to adapt the platforms to the new needs, in particular related to the flare. Due to its greater dimension owing to the increase of platform production capacity, the design of offshore flare systems requires special concerns. Thus, it is important to correctly design the flare in terms of flow and heat transfer to guarantee the safe operation of the platform. Moreover, some radiation blocking technology, such as heat shields, can be useful to reach this goal. The present work introduced two techniques for measuring the emissivity of surfaces, commonly used in the structure of heat shields: a Thermal Sprayed Aluminum (TSA) coating, a Jotatemp1000 coating and a raw naval steel surface. The experimental study was based on two different experimental procedures, coupled with a mathematical model that enabled to calculate the heat transfer by convection and radiation and the emissivity. The first method measured the emissivity with the aid of a thermographic camera at five different temperatures, ranging from ambient temperature to 200°C for each surface. Moreover, for TSA and Jotatemp1000 coatings, the emissivities of a flat plate and tube (both coated) were compared to assess the impact of the curvature in the estimation. The second experiment determined the emissivity by estimating the heat transfer by natural convection and radiation in an annular space between an internal cylinder dissipating 15, 30, 45 and 60 W of heat from an electrical resistance and an instrumented external cylinder. To quantify the effects of natural convection, the tests were performed under three different pressures levels. The first experiment exhibited a significant variation between the values measured in tubes and plates for a same surface showing a strong impact of the geometry. In both experiments, the emissivity of all materials remained constant within the uncertainty range for temperature values higher than 100 °C. However, for the Jotatemp1000 coating and the naval steel, a significant difference was observed in the emissivity values depending of the procedures. Such difference can be related to the hypothesis used in the heat transfer model where conduction was considered negligible.*

Keywords: *Emissivity, Radiation, Annulus, Experiment, Thermography.*

1. INTRODUCTION

The Brazilian energy sector has increased its focus on the use of renewable energies, such as hydraulics and biomass, however its main source is still oil and its derivatives, which add up to almost 35% of the country's internal energy supply. According to EPE (2020), there was an increase of 7.6% in the production of oil and its derivatives between the years 2018 and 2019, in particular an increase of 9.5% in the production of natural gas. This growth is directly linked to the growing contribution of the pre-salt production, which today represents 66.8% of oil production in Brazil (ANP, 2020).

During the oil extraction process, significant amounts of natural gas are also removed from the wells. Although the reinjection of natural gas has increased a lot in recent years (IBP, 2020), all the gas cannot be necessarily transported to the coast, so it is necessary that part of it is burned on the platform itself. Even on platforms that store the extracted gas, this process must be carried out safely. The safety equipment used in this procedure is a structure popularly known as flare, and extensively used in the oil and gas sector for a safe and reliable release of gases and liquids during the normal operational process or in emergency cases. The flare design must meet several technical criteria to define the support

structure. In addition, it is necessary to determine the type of burner that will be used, as well as its sizing and the inclusion of a detailed thermal project (Pagot *et al.*, 2008).

This prior care in planning this equipment is extremely important, since solar irradiation added to the flare can have highly damaging impacts on equipment, pipes, surfaces in general and serious damage to human health (Kim *et al.*, 2014). Poor sizing can also affect the smooth running of field production due to the high surface temperature. To prevent these types of problems, it is common to install security equipment such as the heat shield. These equipment are responsible for blocking the high heat radiation emitted from the flare and in some cases the structure surface of the flare is coated with a material with high emissivity, reducing drastically the temperature on the flare structure (Bader *et al.*, 2008).

Emissivity measurement can be performed directly or indirectly. The direct methods involve the measurement of infrared rays emitted by the studied surface and from this, the emissivity is found. Indirect methods involve measuring some quantity that can be correlated with emissivity such as heat flux, reflectivity, etc.

The present work aims to determine the emissivities of three surfaces, two with coated materials and one raw material. For this, two emissivity measurement methodologies were investigated: direct measurement through thermographic images and indirect measurement assessing the multimode heat transfer (natural convection and radiation) in a annular space. The behavior of the emissivity of each material is analyzed for the same temperature range, compatible with field conditions, determining which material is best suited for the purpose of reducing heat emission by radiation. In the present work, the modeling and equation of the proposed experiment was carried out, the emissivities measured by the two proposed methodologies were compared and the uncertainties estimated.

2. HEAT TRANSFER MODELING

2.1 Radiation

In the present study, the studied surface are considered grey bodies. That means that the emissivity is equal to the absorptivity (Incropera *et al.*, 2007). Moreover, it is necessary to consider the geometry of the surfaces involved to determine the fractions of radiation that each surface is receiving, by calculating the shape factor of one surface in relation to another. Using correlations found in the literature (Holman, 2009), it is possible to determine the shape factors for the geometry of the two coaxial cylinder, where the index 2 refers to the outer cylinder, 1 to the inner cylinder and 3 to the covers:

$$F_{21} = \frac{1}{r} - \frac{1}{\pi r}\left\{cos^{-1}\left(\frac{B}{A}\right) - \frac{1}{2H}\left[f1 \cdot cos^{-1}\left(\frac{B}{rA}\right) + B \cdot sin^{-1}\left(\frac{1}{r}\right) - \frac{\pi A}{2}\right]\right\} \tag{1}$$

$$F_{12} = \frac{A_2}{A_1}F_{21} \tag{2}$$

$$F_{22} = 1 - \frac{1}{r} + \frac{2}{\pi r}tan^{-1}\left(\frac{2\sqrt{f_2}}{H}\right) - \frac{H}{2\pi r}\left[f_3 \cdot sin^{-1}(f_4) - sin^{-1}\left(\frac{f_2 - 1}{r^2}\right) + \frac{\pi}{2}(f_3 - 1)\right] \tag{3}$$

$$r = \frac{r_2}{r_1} \quad ; \quad H = \frac{L}{r_1} \quad ; \quad A = H^2 + r^2 - 1 \quad ; \quad B = H^2 - r^2 + 1$$

$$f_1 = (A+2)^2 - 4r^2 \quad ; \quad f_2 = r^2 - 1 \quad ; \quad f_3 = \frac{\sqrt{4r^2 + H^2}}{H}$$

$$f_4 = \frac{4f_2 + (H^2/r^2)(f_2 - 1)}{H^2 + 4f_2}$$

Where r_1 is the inner cylinder radius, r_2 is the outer cylinder radius and L the cylinder length. Knowing that $F_{11} = 0$ because it is a convex surface and that the sum of all the shape factors of a single surface is equal to 1 (Incropera *et al.*, 2007):

$$F_{13} = 1 - F_{12} \tag{4}$$

$$F_{23} = 1 - F_{21} - F_{22} \tag{5}$$

According to Kreith (1973), the radiation heat transfer in the annular space is described by:

$$Q_{r1} = \frac{\sigma\left({T_2}^4 - {T_1}^4\right)}{\frac{1-\varepsilon_1}{\varepsilon_1 A_1} + R_{eq} + \frac{1-\varepsilon_2}{\varepsilon_2 A_2}} \tag{6}$$

$$R_{eq} = \left[\frac{1}{R_1 + R_2} + \frac{1}{R_3}\right]^{-1} \tag{7}$$

$$R_1 = \frac{1}{A_1 F_{13}} \quad ; \quad R_2 = \frac{1}{A_2 F_{23}} \quad ; \quad R_3 = \frac{1}{A_1 F_{12}} \tag{8}$$

Where $Q_{r1}\ (W)$ is the radiation heat transfer rate for the finite cylinders, $\sigma = 5.67 \times 10^{-8}\ W/m^2 \cdot K^4$ is the Stephan-Boltzmann constant, ε_i the surface emissivity i, $A_i\ (m^2)$ the the area of surface i, R_1 is the thermal resistance between the inner cylinder and the covers, R_2 is the thermal resistance between the outer cylinder and the covers , R_3 the thermal resistance between the outer cylinder and the inner cylinder and R_{eq} the equivalent thermal resistance. For the case where the cylinder length is much larger than the hydraulic diameter ($L >> D_h$), the equation for the radiation heat transfer rate $Q_{r2}\ (W)$ becomes (Incropera *et al.*, 2007):

$$Q_{r2} = \frac{\sigma\left({T_1}^4 - {T_2}^4\right)}{\frac{1}{\varepsilon_1} + \frac{1-\varepsilon_2}{\varepsilon_2}\left(\frac{A_1}{A_2}\right)} \tag{9}$$

2.2 Natural Convection

In order to calculate the emissivity in the annular space, it is necessary to quantify the heat transfers by natural convection and radiation. With the purpose of modeling the natural convection in the annular space, the confined space correlations of parallel plates can be used (Kreith, 1973) :

$$Q_c = h_c A_{lm}\left(T_2 - T_1\right) = \frac{k}{D_h} Nu \cdot A_{lm}\left(T_2 - T_1\right) \tag{10}$$

$$Nu = 1 \quad \Longrightarrow \quad Gr \leq 2000 \tag{11}$$

$$Nu = 0.18 \cdot Gr^{1/4}\left(\frac{D_h}{L}\right)^{1/9} \quad \Longrightarrow \quad 2000 < Gr < 20000 \tag{12}$$

$$Nu = 0.065 \cdot Gr^{1/3}\left(\frac{D_h}{L}\right)^{1/9} \quad \Longrightarrow \quad 20000 < Gr < 1.1 \times 10^7 \tag{13}$$

Where $h_c\ (W/m^2 \cdot K)$ is the coefficient of heat exchange by convection and $A_{lm}\ (m^2)$ the mean logarithm area, Nu the Nusselt number, Gr the Grashof number, $D_h\ (m)$ the hydraulic diameter, $d_{air}\ (kg/m^3)$ the density of air, $g\ (m/s^2)$ the gravitational acceleration, $L\ (m)$ the length of the tube and $\mu\ (Pa \cdot s)$ the viscosity of air.

2.2.1 Knudsen Number

In order to decrease the contributions of natural convection in the heat transfer process, it is recommended to lower the pressure in the cavity to a minimum (vacuum if possible). To define more clearly the impact of the heat transfer by radiation, the creation of a semi-vacuum or vacuum in the annular space reduces the contribution of convection. From this, it is guaranteed that the error propagated by the convection heat transfer calculus is smaller as the calculated heat transfer is more correlated with the radiation. By decreasing the pressure, the convection effect becomes smaller, since there is a greater distance between the molecules. In this case, the mean free path between the molecules must be considered, that is, the average distance two consecutive collision of a molecule. If this path is of the same order of magnitude as the characteristic length (in this case, the distance between the tubes), the problem lies in a regime where the classical formulations of fluid mechanics do not satisfactorily describe the problem and conduction in the fluid should be considered instead of convection. The dimensionless number that determines this regime is called Knudsen Number (Al-Kouz *et al.*, 2016) and its formulation is as follows:

$$Kn = \frac{\eta}{\gamma} = \frac{k_B T}{\gamma\sqrt{2}\pi\delta^2 P} \tag{14}$$

Where, $\eta\ (m)$ is the mean free path between molecules, $\gamma\ (m)$ is the characteristic length at which heat transfer occurs (in this case $(D_i - d_e)/2$), $k_B = 1.38 \times 10^{-23}\ J/K$ is the Boltzmann constant, $T\ (K)$ the fluid temperature, $\delta\ (m)$ the fluid particle diameter and $P\ (Pa)$ the absolute pressure. The continuous regime is determined when the Knudsen number is lower than $Kn \leq 0.01$, as described in (Al-Kouz *et al.*, 2016). As noted in the equation 14, the mean free path between the molecules is directly proportional to the temperature and inversely proportional to pressure, the other parameters are constant for a given work fluid. Therefore, the worst case which correspond to the highest temperature and lowest pressure, that is, the highest η. The maximum expected temperature in the experiment is $573\ K$ and the lowest pressure is $0.1\ atm$. For these values:

$$Kn = \frac{1.381 \times 10^{-23} \cdot 673}{10132.5 \cdot (3.5 \times 10^{-10})^2 \cdot \pi\sqrt{2} \cdot (0.04763 - 0.0254)}$$

$$Kn \approx 5.2 \times 10^{-5}$$

The value found for the Knudsen number is far below the limit of the continuity regime even in the worst case, so there are no concerns about the effects of conduction on the fluid.

2.3 Problem Modeling - Multimode Heat Transfer

Based on the model presented in the previous sections, a mathematical equation of the present case can be formulated:

$$Q_t = Q_c + Q_{ri} = A_{lm} \cdot h\,(T_1 - T_2) + C_{ri} \cdot \left({T_1}^4 - {T_2}^4\right) = C_c \cdot \Delta_h T + C_{ri} \cdot \Delta_4 T \tag{15}$$

$$C_c = A_{lm} \quad ; \quad C_{r1} = \frac{\sigma}{\left(\frac{1-\varepsilon_1}{\varepsilon_1 A_1}\right) + R_{eq} + \left(\frac{1-\varepsilon_2}{\varepsilon_2 A_2}\right)} \quad ; \quad C_{r2} = \frac{\sigma}{\frac{1}{\varepsilon_1} + \frac{1-\varepsilon_2}{\varepsilon_2}\left(\frac{A_1}{A_2}\right)}$$

Where Q_c, Q_{r1} and Q_{r2} are respectively the heat rate due to natural convection, the radiation for the finite cylinder hypothesis and the radiation for infinite cylinders. The constants C_c, C_{r1} and C_{r2} are related to the same quantities respectively.

2.4 Determination of Quantities

For the calculation of convection and radiation heat transfer, it is necessary to use other quantities, such as: density, thermal conductivity, viscosity, heat exchange coefficients, etc. Some of these quantities can be estimated in a simple way, as is the case of density, others however require a slightly more refined analysis. According to (Sonntag and Borgnakke, 2009):

$$d_{ar} = \frac{P}{RT} \tag{16}$$

$$c_p = 1050 - 0.365T + 0.00085T^2 - 0.00000039T^3 \tag{17}$$

$$c_v = c_p - R \tag{18}$$

Where $V\ (m^3)$ is the volume, $m\ (kg)$ the mass of the gas, $P\ (Pa)$ the absolute pressure, $T\ (K)$ the absolute temperature, $R\ (J/mol \cdot K)$ the universal constant of ideal gases, $c_p\ (J/kg \cdot K)$ is the specific heat at constant pressure and $c_v\ (J/kg \cdot K)$ the specific heat at constant volume. Through the model presented in (Lemmon and Jacobsen, 2004) the viscosity $\mu\ (Pa \cdot s)$ and thermal conductivity $k\ (W/m \cdot K)$ can be estimated using the correlations for air presented in Lemmon and Jacobsen (2004).

3. MATERIALS AND METHODOLOGY

The determination of emissivity was carried out from two experiments and the calculated values are compared. The first experiment consisted in the direct measurement of emissivity using a thermographic camera. In this, measurements of flat coated plates with the materials were investigated and also coated tubes with the same materials to quantify the impact of the curvature. The second experiment was based on the indirect measurement of emissivity by gauging the heat exchange by radiation and natural convection in an annular space, with the inner cylinder coated with the material to be investigated. In each experiment, the emissivities of three surfaces were measured: a surface with TSA coating, another with Jotatemp1000 coating and finally a raw steel surface for marine use.

3.1 Measurement on Plane Plates with Thermographic Camera

3.1.1 Experimental Apparatus

For this experiment, the following materials were used: two ASTM A36/SAE 1006/20 steel sheets in dimensions $20cm \times 20cm \times 1cm$; two K-type thermocouples for the plane plates; Jotatemp 1000 coating; thermal Sprayed Aluminum coating; two 63/37 brass tubes of 2" outside diameter and $1/8$" wall thickness; one ASTM A131M steel tube with grades AH36 / DH36 / EH36 and 2" outside diameter and $1/8$" wall thickness; two modular ceramic electrical resistors with $1\ kW$ of power; nine K-type thermocouples for the tubes (three in each); temperature controller; temperature measurement display; FLIR thermographic camera model A655sc with $640x480$ pixels resolution and spectral range from $7.5\ \mu m$ to $14.0\ \mu m$. The thermographic camera was installed and positioned as shown in the figures 1b e 1a.

(a) Temperature controller display

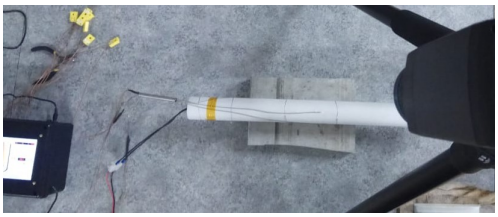

(b) Thermographic camera positioning

Figure 1: Temperature display and experimental apparatus positioning

3.1.2 Experimental Methodology

For the measurement of emissivity using the thermographic camera, 5 surfaces were prepared: a steel plate covered with Jotatemp1000, a steel plate covered with TSA, a brass tube covered with Jotatemp1000, a brass tube covered with TSA and a tube of naval steel. The TSA and Jotatemp1000 tubes were used for comparison with the plates, this way it is possible to gauge the effects of surface curvature. The plates have dimensions of $40\ cm$ by $40\ cm$, were instrumented with thermocouples close to their center and heated using a rectangular-shaped electrical resistor. Tubes are $60\ cm$ long with 2" outside diameter with $1/8$" wall thickness and were heated using a modular cylindrical resistance. Three thermocouples

were placed in them, spaced 100 mm apart and with an angular distance of 120. In this case, the unique thermocouple used for the measurement is the central one, the other two will be used to guarantee the homogeneity of temperature on the surface. For this experiment, five temperatures were chosen: $25°C$ (ambient temperature, used as a calibration parameter), $50°C$, $100°C$, $150°C$ and $200°C$. These temperatures will be reached with the aid of a temperature controller and a display.

The thermographic camera uses a standard emissivity to determine surface temperature based on the wavelengths it receives. By measuring the experimental temperature with the thermocouple, it is possible possible to determine the real emissivity. The experimental procedure follows these steps: 1. The thermographic camera is calibrated at room temperature with a material of known emissivity, a black body, for example; 2. The surface under investigation is placed on the table below the thermographic camera; 3. On the display, the desired temperature must be selected, after a period of time the controller maintains the thermal balance; 4. With the thermographic camera pointed at the surface (near the thermocouple), the actual temperature obtained by the thermocouple must be adjusted so that the equipment can calculate the corresponding emissivity; 5. Repeat steps 3 and 4 until emissivity measurements are obtained for the temperatures of $25°C$, $50°C$, $100°C$, $150°C$ and $200°C$; 6. Perform the entire procedure for the five surfaces.

3.2 Measurement in the Annular Space

3.2.1 Experimental Apparatus

For this experiment, the equipment used to measure the emissivity of the surfaces were: two 63/37 brass tubes of 2" outside diameter and $1/8$" wall thickness; one ASTM A131M steel tube with grades AH36 / DH36 / EH36 and 2" outside diameter and $1/8$" wall thickness; one 63/37 brass tube of 4" outside diameter and $1/8$" wall thickness; two modular ceramic electrical resistors with power equal to 1 kW; two teflon plates; o'rings for the inner tubes - VITON with $d = 1\frac{7}{8}$" ; $e = 2.5\ mm$; o'rings for the outer tube - VITON with $d = 3\frac{7}{8}$" ; $e = 2.5\ mm$; sealing o-rings with $d = 9.5\ mm$ and $e = 4\ mm$; two steel sheets; four screws; twelve K-type thermocouples; Jotatemp 1000 coating; thermal spray aluminum coating; power controller; temperature measurement display; Honeywell pressure transducer - Model FPA; Quimis vacuum pump - Model Q-355B. It is important that the edge effects are considered and therefore the chosen length of the tubes was determined as $L \geq 12 \cdot D_h$:

$$D_h = 44.46\ mm$$

$$L_{min} = 53.35\ cm$$

A value of 60 cm was taken for the length of the tubes to be higher than this calculated value. The equipment was installed and positioned as shown in the figures 2a e 2b.

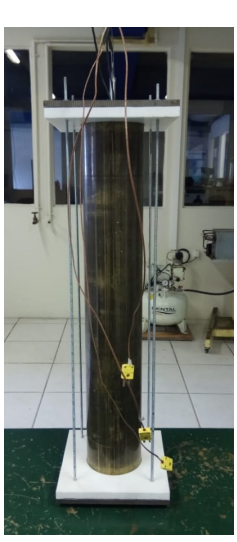

(a) Frontal view of the apparatus

(b) Isometric view of the apparatus

Figure 2: Experimental apparatus for the measurement of emissivity in the annular space

3.2.2 Experimental Methodology

In this experiment, four tubes with $1/8$" wall thickness were used. The outer brass tube has a diameter of $D = 4$", the other three inner tubes have a diameter of $d = 2$" and are covered with the materials that the emissivity should be estimated. The inner tubes are instrumented with thermocouples on the coating side surface (where the cover is) to measure the surface temperature. The thermocouples were arranged at a distance of $100\ mm$ from each other, with the central thermocouple positioned at $L/2 = 300\ mm$. In addition, they were separated at an angle of $120°$ to guarantee the variability of measurements. Small holes (non-through holes) are made on the external surface and the thermocouples placed at a certain depth to allow the temperature measurement of the inner walls of this tube. The thermocouples were placed with an identical spacing to the inner tubes. As the tube is $600\ mm$, the thermocouples were distributed as follow: $T_1 = 200\ mm$;$T_2 = 300\ mm$; $T_3 = 400\ mm$; $\theta_1 = 0°$; $\theta_2 = 120°$; $\theta_3 = 240°$.

In order to reduce the conduction through the covers, Teflon thermal insulation are used. In addition, two more diametrically opposed holes are made in the top cover, for the passage of the thermocouple wires and the inlet of the vacuum pump. For each material, the same equipment assembly procedure is followed: 1. One of the inner tubes is selected to determine the emissivity of the material in its covering; 2. Ceramic heater is fitted to the chosen inner tube; 3. The o-rings are inserted in the grooves of the Teflon plates for the correct sealing of the equipment during the pressure reduction process; 4. Fit the outer tube and the inner tube into the grooves of the Teflon caps, passing the metal tube of the thermocouples through the hole in the cap; 5. Then, the two steel plates are positioned outside the Teflon covers; 6. The screws are passed through the holes in the steel plates and in the Teflon plates and tightened with nuts so that the seal is guaranteed; 7. Connect the thermocouples to the power control display; 8. Attach the vacuum pump to the second hole of the teflon plate with the help of a spike and in parallel with a pressure transducer. A test is performed to ensure there are no leaks at this step.

With the assembled equipment, measurements of internal and external temperature can be carried out for different powers in the internal resistance. The analysis of convection effects is performed by repeating the experiment for three different pressures: $1\ atm$, $0.5\ atm$ and $0.1\ atm$. This results in a larger set of results, allowing the analysis of uncertainty estimation for each pressure. Four powers were used as the basis for heating the inner tube: $15\ W$, $30\ W$, $45\ W$ and $60\ W$. As the temperature of the inner tube increases, heat is transferred to the outer tube by natural convection and radiation. After attaining the steady state, the equilibrium temperatures for the inner and outer cylinder were recorded and the equations and correlations presented in the section 2.6 are used to find all the necessary auxiliary quantities. Then, the heat transfer rates and consequently the emissivity of the surfaces following the experimental procedure: 1. If necessary, the vacuum pump is activated to reach the determined pressure and maintained with the aid of a valve; 2. Turn on the ceramic resistance at one of the powers previously presented and wait until thermal equilibrium; 3. The results presented on the display are recorded for the three external and internal temperatures; 4. Steps 3 and 4 must be repeated for each power until at least 3 measurements are obtained at each power; 5. It is estimated the natural convection and, consequently, the radiation; 6. With the assumed value of the radiation, data analysis and treatment are performed and using these results it is possible to estimate the emissivity from two calculations; 7. Calculating point-to-point emissivity with radiation values using the equation 6; 8. Using matlab's fit command to interpolate an equation of the response surface as shown in equation 15.

4. RESULTS DISCUSSION

4.1 Thermographic Camera Results

After performing the steps described in section 3, the following emissivity values were determined for the three materials:

Table 1: Plate and Tube Emissivity with TSA Coating

Properties	**TSA Plate**					**TSA Tube**				
$T\ (°C)$	26	53	100	150	200	25	50	100	150	200
ε	0.839	0.463	0.405	0.396	0.390	1.000	0.450	0.294	0.279	0.276

Table 2: Plate and Tube Emissivity with Jotatemp 1000 Coating

Properties	**Jotatemp 1000 Plate**					**Jotatemp 1000 Tube**				
$T\ (°C)$	25.5	50	102	150	200	28	50	100	152	193
ε	0.742	0.963	0.927	0.956	0.961	0.640	0.882	0.871	0.867	0.877

Table 3: Raw Naval Steel Emissivity

Properties	**Naval Steel Tube**				
$T\ (°C)$	28.5	51	100	150	200
ε	0.611	0.643	0.700	0.716	0.750

The uncertainty associated with the thermographic camera is directly related to the uncertainty of the temperature measurement, as the emissivity is found from the temperature that is set in the equipment. The temperature has an uncertainty of $\delta T = \pm 0.5\ °C$, which generates an uncertainty in emissivity of approximately $\delta\varepsilon = \pm 0.030$ for all calculated values. It is important to note that the thermographic camera measurement values on both the plate and the tube at room temperature are not representative of the actual emissivity values. This occurs because thermocouples have a very large uncertainty in measuring surface temperature close to room temperature, so the emissivity ends up varying a lot in these cases.

As seen in the tables 1 and 2, the emissivity values were different for the plate and the tube. This is probably due to the fact that the curvature of the tube causes a reflection of the rays in directions out of the scope of the thermographic camera reading field. Thus, the amount of radiation received back by the equipment is smaller, giving the impression of a lower emissivity than in the case of the flat plate. In the case of Jotatemp the measurements on the tube represented 90% the values obtained on the plate. However, in the case of the TSA the emissivity values measured on the tube were around 70% of those on the plate, this occurrence is due to the fact the aluminum surfaces have a higher reflectivity than the other surfaces.

Furthermore, in the 2 and 3 tables, the emissivity values increase with temperature, for the TSA the opposite occurs as shown in table 1. These two behaviors are consistent with the expected of these materials as shown in Incropera *et al.* (2007).

4.2 Annular Space Results

4.2.1 Finite Cylinder Hypothesis

Table 4: Mean Emissivity for the Finite Cylinder Hypothesis

	TSA		**Jotatemp**		**Naval Steel**	
Pressure	ε_{TSA}	$\delta\varepsilon_{TSA}$	ε_{Jot}	$\delta\varepsilon_{Jot}$	ε_{steel}	$\delta\varepsilon_{steel}$
$1\ atm$	0.257	0.030	0.421	0.056	0.309	0.037
$0.5\ atm$	0.260	0.026	0.463	0.058	0.335	0.037
$0.03\ atm$	0.375	0.039	0.589	0.085	0.462	0.056
Surface	0.404	0.054	0.697	0.115	0.546	0.076

The emissivity values measured in this experiment are below those measured in the previous section. One possibility for this fact would be that heat transfer by conduction in the two covers is not negligible as assumed in the experiment. It is also necessary to consider the hypothesis that the insulating covers do not have a re-irradiating behavior, this last factor is analyzed in the next section when the hypothesis of infinite cylinders is considered. It is important to note that the greatest discrepancies occur at higher pressures, that is, in regimes where natural convection has a greater influence on the heat exchange process. Note that, for values at the lowest pressure ($0.03\ atm$), the values of TSA emissivity were about 90% of the values found in the thermographic camera and within the uncertainty range the values are consistent with each other. As for the case of Jotatemp and naval steel, there is a greater discrepancy, it is possible that the assumption of negligible conduction has generated lower convection and radiation values than the real ones, resulting in lower emissivity values. In relation to the table **??**, it is possible to notice a better approximation of the results in relation to the thermographic camera experiment. In the case of marine steel and Jotatemp, there is still a discrepancy due to the assumption that the conduction has been disregarded. The R^2 were all very high, the lower being $R^2 = 0.9764$, that implies the modeling and fitting done by matlab represents the sample satisfactorily as shown in figure 3.

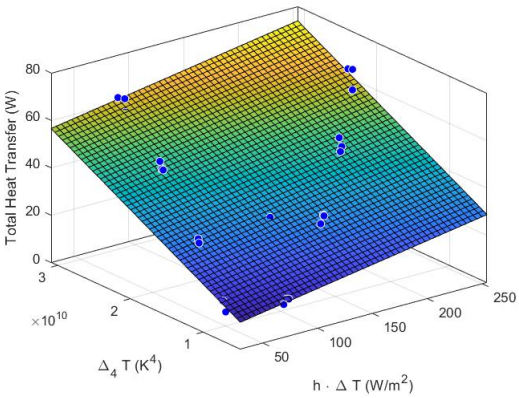

Figure 3: Response surface of TSA coating for the finite cylinder hypothesis

4.2.2 Infinite Cylinder Hypothesis

Table 5: Mean Emissivity for the Infinite Cylinder Hypothesis

	TSA		**Jotatemp**		**Naval Steel**	
Pressure	ε_{TSA}	$\delta\bar{\varepsilon_{TSA}}$	ε_{Jot}	$\delta\bar{\varepsilon_{Jot}}$	ε_{steel}	$\delta\bar{\varepsilon_{steel}}$
$1\ atm$	0.256	0.031	0.418	0.062	0.308	0.039
$0.5\ atm$	0.259	0.027	0.459	0.066	0.333	0.040
$0.03\ atm$	0.375	0.044	0.584	0.099	0.459	0.065
Surface	0.402	0.059	0.690	0.135	0.541	0.088

The values of emissivity found adopting this hypothesis were very close to those presented above, with a variation of less than 2% in the average value. Thus, it can be observed that the radiation effects due to the cover can be practically neglected, since in the hypothesis of infinite cylinders covers are not considered. Like in the previous model, the R^2 related to the surface found on matlab were close to 1 (ranging between 0.97664 and 0.9892), meaning the model represents the points satisfactorily. Similarly, there is still a significant discrepancy for the coating of Jotatemp and the marine steel surface. Therefore, it is likely that the conduction trough the covers affected the values of radiation and convection, causing a discrepancy in emissivity. The values found by the parameterization made with the matlab fit command were also closer to the measurement performed by the thermographic camera as demonstrated in figure 4.

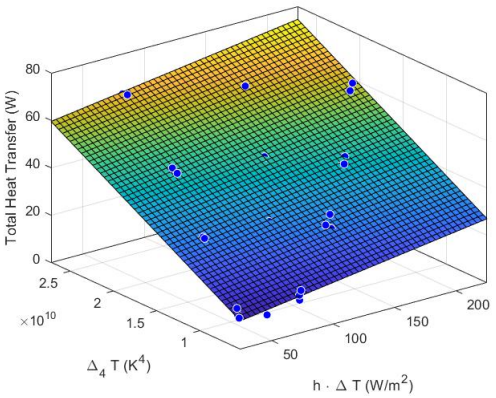

Figure 4: Response surface of naval steel for the infinite cylinder hypothesis

5. CONCLUSION

The present work aimed to measure the emissivity of 3 surfaces by 2 experiments, one of direct measurement using an infrared radiation thermographic camera and another of indirect measurement based on the heat transfer in an annular. In this second experiment, two approaches were used to represent the heat transfer by radiation within the cavity for different hypothesis of radiation heat quantification.

As shown in the previous section, the emissivity values of TSA are all very close and within the experimental uncertainty, this is probably due to the fact that the emissivity of TSA is lower than the other compounds. As for Jotatemp1000 and marine steel, there was a significant discrepancy between the values found by the thermographic camera experiment and the measurement in the annular space. It is likely that this behaviour is due to the fact that thermal conduction is not negligible in the experiment, even with thermal insulation. This loss results in lower stability temperatures than in the case of total insulation, resulting in an overestimation of convection heat and, consequently, an underestimation of radiation. The radiant heat has a dependency on $\left({T_1}^4 - {T_2}^4\right)$, while the convection heat $(T_1 - T_2)$, hence the consequences of this smaller temperature affects radiation more than convection.

Moreover, for both modeling of the annular space method the values are very close. This fact reinforces the assumption that caps do not significantly influence radiation. This confirms that the design of the apparatus was done properly and the edge effects were not relevant. In both experiments, the emissivity calculated at the lowest temperatures showed the greatest discrepancy in relation to the others, this can be explained by the fact that thermocouples have a greater measurement uncertainty at temperatures closer to ambient. Furthermore, it is noticeable that, for all material the emissivity remains practically constant for values equal to or greater than $100\ ^{\circ}C$.

In the thermographic camera experiment, there was a discrepancy in the measurements when measuring the emissivity of flat or curved surfaces, this is probably due to the fact that the thermographic camera does not capture some rays reflected by the curved surface, resulting in a lower radiation value and consequently lower emissivity in all cases. For this reason, the more robust methodology to calculate the emissivity for the curved (ie, non flat) surfaces within the temperature 25-200ºC is the determination of the heat transfer within the annular space. In order to define the most appropriate coating for the structure of the heat shield, it is clear from the results that the best material for this application would be the Jotatemp1000 coverage, since this has the highest emissivity in all experiments.

For future work, it is interesting to investigate more materials, as well as other temperature and pressure regimes. Moreover, it is essential to use other models to calculate conduction losses, in this way it can be possible to determine which effect these losses affected the results.

6. ACKNOWLEDGEMENTS

The authors are indebted to CNPq/MCT and CAPES for the financial support to the Department of Mechanical Engineering (DEM) at the Pontifical Catholic University of Rio de Janeiro (PUC-Rio). The authors gratefully acknowledge Petróleo Brasileiro SA for the financial support within the scope of a R&D&I research project regulated under the terms of RT n.03/2015, referring to the Research, Development and Innovation Clause of the Brazilian National Agency for Petroleum, Natural Gas and Biofuels (ANP).

7. REFERENCES

Al-Kouz, W., Alshare, A., Alkhalidi, A. and Kiwan, S., 2016. "Two dimensional analysis of low pressure flows in the annulus region between two concentric cylinders".

ANP, 2020. "Produção de petróleo bate recorde e ultrapassa 1 bilhão de barris".

Bader, A., Baukal, C. and Bussman, W., 2008. "Selecting the proper flare systems". *Brazilian Petroleum, Gas and Biofuels Institute*.

EPE, 2020. "Brazilian energy balance 2020, final report".

Holman, J., 2009. *Heat Transfer*. McGraw-Hill.

IBP, 2020. "Evolução da reinjeção de gás natural no brasil entre 2010 e 2019".

Incropera, F., Dewitt, D., Bergman, T. and Lavine, A., 2007. *Fundamentals of Heat and Mass Transfer*. Editora John Wiley & Sons.

Kim, S., Park, S., Lee, J., Seo, J., Kim, B., Ha, Y., Paik, J. and Heo, T., 2014. "Experimental study of the reduction of high temperatures and radiation using heat shields associated with flare towers of offshore oil and gas platforms".

Kreith, F., 1973. *Principles of Heat Transfer*. Intext Educational Publishers.

Lemmon, E. and Jacobsen, R., 2004. "Viscosity and thermal conductivity equations for nitrogen, oxygen, argon, and air". *International Journal of Thermophysics*.

Pagot, P., Burmann, C., Araujo, P. and Motomura, T., 2008. "Offshore production flares – a petrobras review". *Rio Oil & Gas Expo and Conference 2008*.

Sonntag, R. and Borgnakke, C., 2009. *Fundamentals of Thermodynamics*. Editora Blucher.